Nat. Hazards Earth Syst. Sci., 11, 267–272, 2011
www.nat-hazards-earth-syst-sci.net/11/267/2011/
doi:10.5194/nhess-11-267-2011
© Author(s) 2011. CC Attribution 3.0 License.

Natural Hazards and Earth System Sciences

New findings on the effects of the İzmit M_w=7.4 and Düzce M_w=7.2 earthquakes

H. S. Kutoglu[1], **R. N. Celik**[2], **M. T. Ozludemir**[2], **and C. Güney**[2]

[1]Zonguldak Karaelmas University, Department of Geodesy and Photogrammetry, Hazard Monitoring & Research Laboratory, 67100, Zonguldak, Turkey
[2]Istanbul Technical University, Department of Geomatics, IGS ISTA Satellite Observation and Processing Laboratory, Maslak, Istanbul, Turkey

Received: 31 March 2010 – Revised: 18 October 2010 – Accepted: 19 October 2010 – Published: 2 February 2011

Abstract. The 17 August 1999 İzmit $M_w = 7.4$ and the 12 November 1999 Düzce $M_w = 7.2$ earthquakes caused a 150 km long surface rupture in the western part of the North Anatolian Fault. The coseismic slips along the fault line and the trace of the surface ruptures were studied in detail in Barka (1999), Reilinger et al. (2000), Cakir et al. (2003a, b) and Ergintav (2009) after the earthquakes. However, the basin to the east of Sapanca Lake was a black hole for all investigations because there was no geodetic network and no significant deformation that could be obtained by using InSAR techniques. In this study, findings on the abovementioned basin have been reinterpreted through a GPS network newly explored. This interpretation shows coseismic slips of between 2–3 m, and links the surface rupture to the main branch of the North Anatolian Fault (NAF) in the east Sapanca basin.

1 Introduction

The 17 August 1999 İzmit $M_w = 7.4$ event was the most destructive earthquake produced by the 1500 km long North Anatolian Fault (NAF) system. The total length of the fault rupture due to this earthquake was about 110 km. The region hit by the earthquake is the industrial heartland of Turkey as well as the most densely populated region. According to official records, the earthquake caused 18 000 deaths, 45 000 injuries and displaced more than 250 000 people. Approximately 214 000 residential units and 30 500 business units were lightly to heavily damaged (USGS, 2000).

Correspondence to: H. S. Kutoglu
(kutogluh@hotmail.com)

The 12 November Düzce $M_w = 7.2$ earthquake occurred three months after the İzmit earthquake. This earthquake produced a fault rupture of 30 km, as seen in a green rectangular in Fig. 2. Two hundred buildings were heavily damaged, 550 people lost their lives and over 3000 people were injured due to earthquake (KOERI, 2010).

Coseismic and postseismic deformations caused by these earthquakes were studied by different researchers using different techniques. First, Barka (1999) reported the maximum coseismic deformations of around 4–5 m along the four segments broken by the İzmit earthquake by means of field reconnaissance (see Fig. 1). Studies based on geodetic techniques, such as GPS and InSAR, resulted in maximum coseismic slips of 5.7 m on the western İzmit segment and the West Sapanca segment, and the maximum postseismic surface slip of 5 cm prior to the November 1999 Düzce earthquake (Reilinger et al., 2000; Cakir et al., 2003a). The maximum coseismic slip of the November Düzce earthquake was estimated at about 4 m around the mid point of the 30 km surface rupture (Cakir et al., 2003a). The postseismic deformations after the Düzce event were studied in Cakir et al. (2003a) and Ergintav et al. (2009).

Common to all above-mentioned studies was that no reliable result could be obtained for the coseismic effects between the eastern Sapanca segment and the more northeast trending Karadere segment (see Fig. 2). Figure 3 displays the interferograms obtained from the InSAR study by Cakir et al. (2003b). The subsequent Fig. 3a shows the interferogram of the İzmit earthquake deduced from ERS1 data pairs acquired on 12 August and 16 September 1999 and Fig. 3b shows the interferogram deduced from ERS 2 data pairs acquired on 13 August and 17 September 1999. As for Fig. 3c, it is the phase difference between the ERS1 and ERS 2 interferograms. In the figures, one interferogram

Published by Copernicus Publications on behalf of the European Geosciences Union.

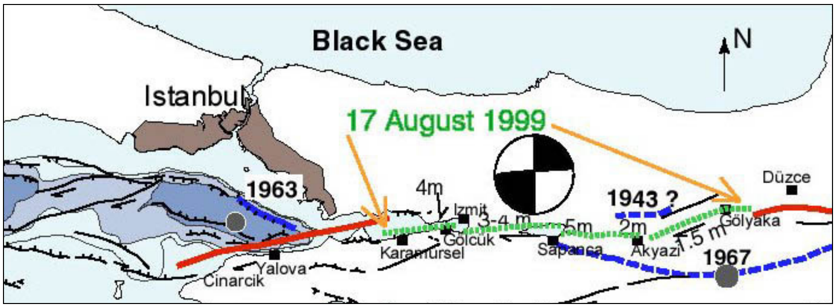

Fig. 1. The map shows the extent of the 1999 rupture (dotted green lines) and the 1943, 1967 and 1963 ruptures (blue lines) and the segments that increased stress (red lines) (Barka, 1999).

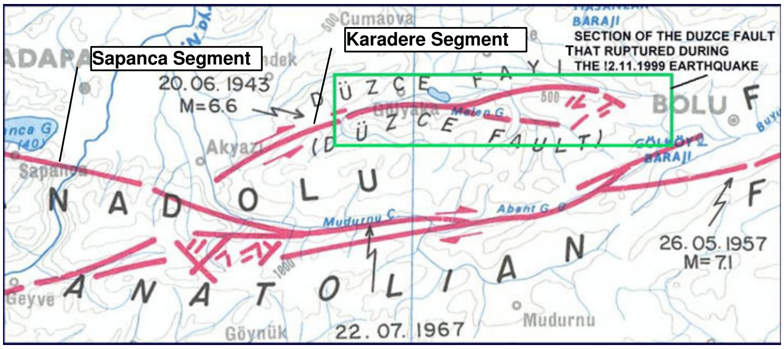

Fig. 2. Surface rupture of the 12 November Düzce earthquake, about 30 km, in the green rectangular (KOERI, 2000).

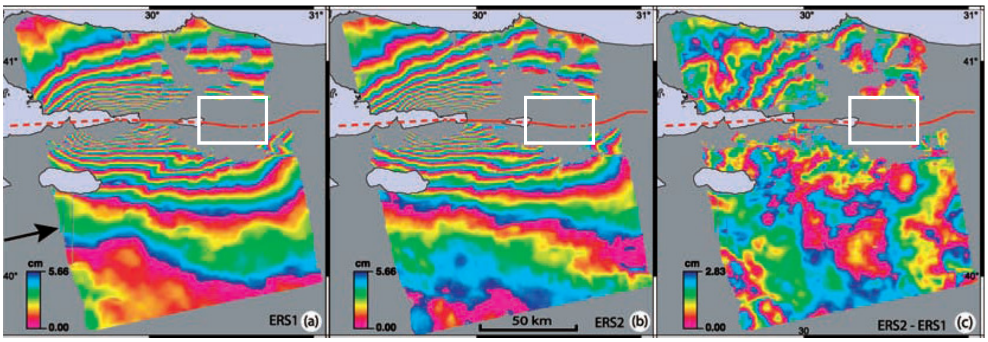

Fig. 3. Interferograms of the İzmit earthquake from ESA satellites ERS1 (12 August–16 September 1999) and ERS2 (13 August–17 September 1999). There is no significant interferogram obtained in the east of Sapanca Lake (from Cakir et al., 2003b).

fringe corresponds a range change of 2.8 cm. As seen from Fig. 3a and b, there are significant phase interferograms of deformation obtained along the ruptured fault line except for the area determined by the white rectangle. Since the displacement associated with the right lateral strike slip occurs in the East-West direction, the fringes in the figures are nearly symmetric and parallel to the fault line. The area surrounded with white rectangle corresponds to the Sakarya basin that is the area of interest of this study. For the area, steep slip gradient, rough topography and water content in the soils are counted as possible reasons of obtaining no interferogram (Cakir et al., 2003b).

There was also no geodetic network in this area especially designed for tectonic monitoring purposes. However, there was a GPS network designed for national mapping purposes, and fortunately that network was observed twice in 1998 and 2001, just before and just after both İzmit and Düzce earthquakes. Due to the purpose of the network, the horizontal positioning accuracy of control stations of the network are ±3 cm (Aliosmanoğlu, 2002; Çelik et al., 2003). Therefore, thanks to this network, the total effects of both 1999 earthquakes in the area between the eastern Sapanca and Karadere can be reinterpreted, and the gaps in the former studies might be completed based on the results obtained in

Fig. 4. Sakarya geodetic control network. Triangles display the network control stations. Stars show the location of the earthquakes. Solid white lines represent the fault lines (satellite image from Google Earth).

this study. It is clear that the magnitude of displacements occurred due to the earthquake is much larger than the accuracy of the network's control stations.

2 Sakarya geodetic control network

Sakarya geodetic control network comprising 22 control stations was established in 1998 for densifying the national geodetic network in order to produce a large scale map of the Sakarya region that is indicated as the white rectangle in Fig. 3. This network was observed using GPS in static mode with an average of one hour sessions, and processed using LEICA SKI-Pro software. During the post-process step, independent baselines between the network stations were solved. The default SKI-Pro processing strategies have been used for baseline solution. One of the main processing criteria is 0.075 m for checking coordinate differences for a station that was obtained from two different baseline solutions based on network geometry. Finally, coordinates of control stations were computed by least square adjustment with respect to the free network adjustment principle (Aliosmanoğlu, 2002; Çelik et al., 2002).

The above-mentioned network covers a 50 km by 30 km area in the West-East and North-South directions between the eastern shore of Sapanca Lake and Hendek town, and surrounds the segments of the North Anatolian Fault in this basin. The 1999 $M_w = 7.4$ İzmit earthquake occurred closed to the western side of the network, and $M_w = 7.2$ Düzce earthquake occurred close to the eastern side. The centre of the İzmit earthquake is 27 km from the eastern end of the network, and the centre of the Düzce earthquake is 28 km from the western end of the network; the earthquake centres are 40 and 60 km away from the geometric centre of the network, respectively. In brief, the Sakarya network is located in between the earthquake centres. For this reason, a new GPS campaign was carried out in 2001 to obtain the post-earthquake coordinates of the site control stations.

Initially the 2001 GPS observations were processed and adjusted in the same way as 1998. A four parameters Helmert transformation was applied between the 1998 and 2001 networks to determine stable control stations of the network after the earthquake. This resulted in two control stations in the northern section of the network, G240068 and G240067, see Fig. 4. The most northern control station G240068 was chosen as "datum point", and the observations in the periods of both 1998 and 2001 were readjusted in respect of the minimally constrained adjustment principle.

3 Analysis of the networks and results achieved

Magnitudes of surface deformations at each control stations shown in Table 1 are attained when the coordinates obtained from both observation periods are compared with each other. The deformations obtained are illustrated by using arrows

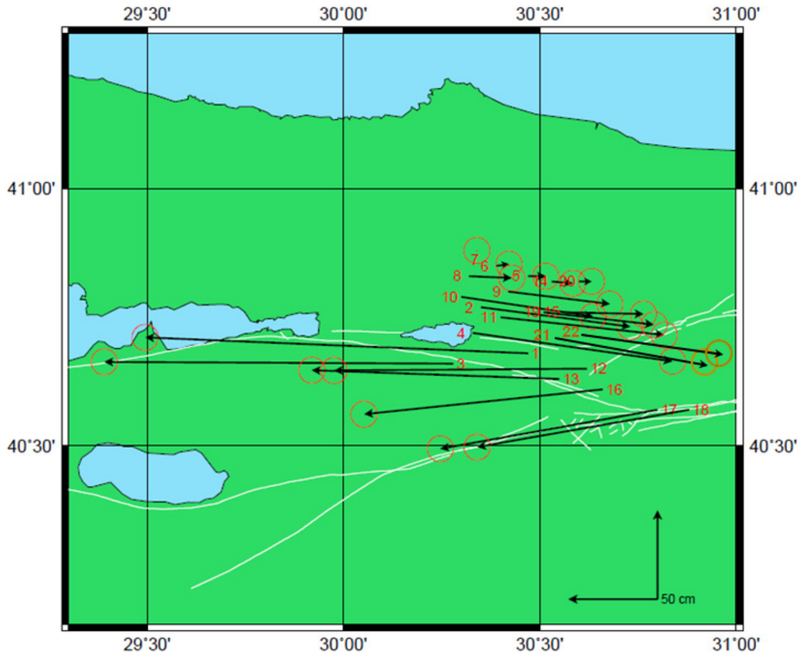

Fig. 5. Surface deformations of Sakarya geodetic control network.

with the positioning error circles at their end (±3 cm) in Fig. 5. As seen in Fig. 5, the deformation is increasing towards the fault lines, which were also observed during surface search in the field after the İzmit event. The maximum displacement in the East component is 2.15 m, and it is at station G240026 that is also named as station 1 in Fig. 5. As is clearly seen in Fig. 5, the deformation on the northern side of the fault is in an easterly direction, whilst the deformation on the southern side is in a westerly direction. Both of these characteristics are consistent with the coseismic deformation behaviour of a right lateral strike slip fault as is of the NAF. Overall, absolute displacements on the North components indicate that the block represented by the network, relative to the stable station G240068, appears to have slipped towards the south, an average of 7.5 cm.

Figure 6 displays the displacement field model based on the deformation at the network stations. The contour lines are compressed in the western central section of the network and enlarging towards the eastern and western sides of the study area. This means the deformation rates on the western and eastern sides are larger than the deformation in the central area. Also, one of the obvious features is the steepness of the deformation gradient in the central section.

Based on the deformation rates, the total surface displacement around the fault line is about 3.10 m in the east bank of Sapanca Lake, decreasing to about 1.8 m in the centre, and increasing to about 2 m in the south-east part of the network. Earlier studies (Barka, 1999; Reilinger et al., 2000; Cakir et al., 2003a; Ergintav et al., 2009) showed that the surface rupture of the Düzce earthquake was limited to

Table 1. Surface deformations of the Sakarya network. Number of control stations are used in both standard and sequential form for constituting a clearer view on figures.

Control Station No*			Displacements in meters	
			Easting	Northing
G240068	→	7	0.00	0.00
G240067	→	6	0.07	0.01
G240065	→	5	0.10	0.00
G250049	→	14	0.12	–0.01
N.7243	→	20	0.00	0.07
G240069	→	8	0.24	–0.01
G240071	→	9	0.57	–0.07
G240075	→	10	0.74	–0.11
G240032	→	2	0.84	–0.11
G240079	→	11	0.92	–0.10
N.7220	→	19	0.62	–0.07
G250054	→	15	0.45	–0.01
G240043	→	13	1.12	–0.16
G240026	→	1	–2.15	0.09
G250043	→	4	–1.39	0.05
G250040	→	12	–1.42	–0.01
G250057	→	16	–1.34	–0.14
G250058	→	17	–1.22	–0.22
G250059	→	18	–1.19	–0.21
G240039	→	3	–1.96	0.01
G250067	→	21	0.60	–0.16
G250069	→	22	0.52	–0.05

* Number of control stations are used in both standard and sequential form for constituting clearer view on figures.

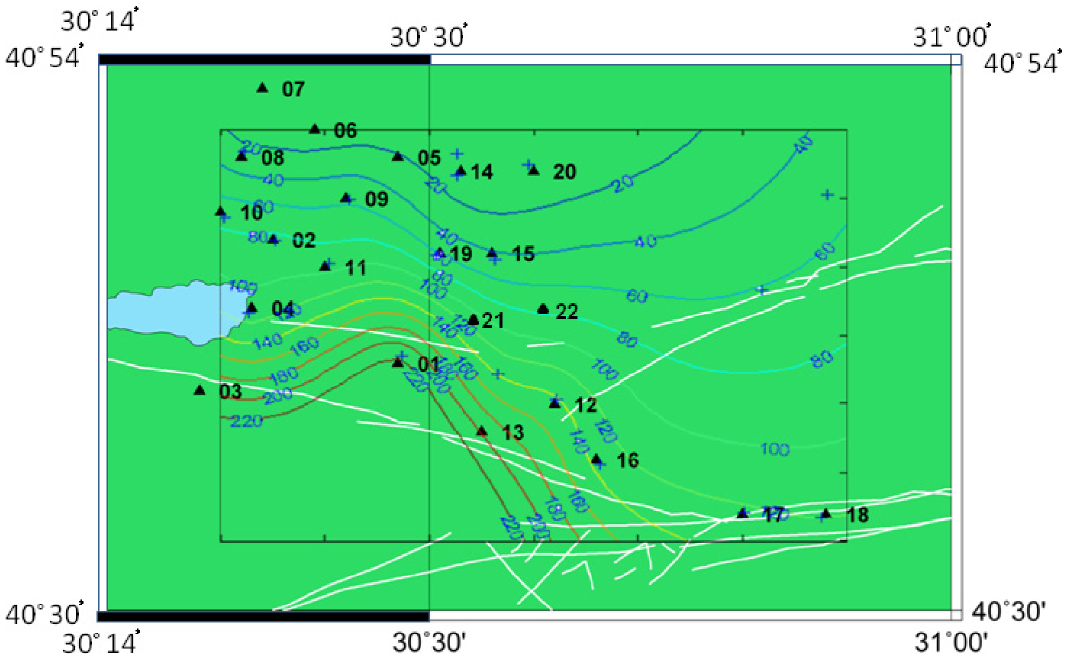

Fig. 6. Displacement field model. Absolute values of deformations are applied for modelling. Contours obtained by extrapolation are removed. Units of deformations are in metres.

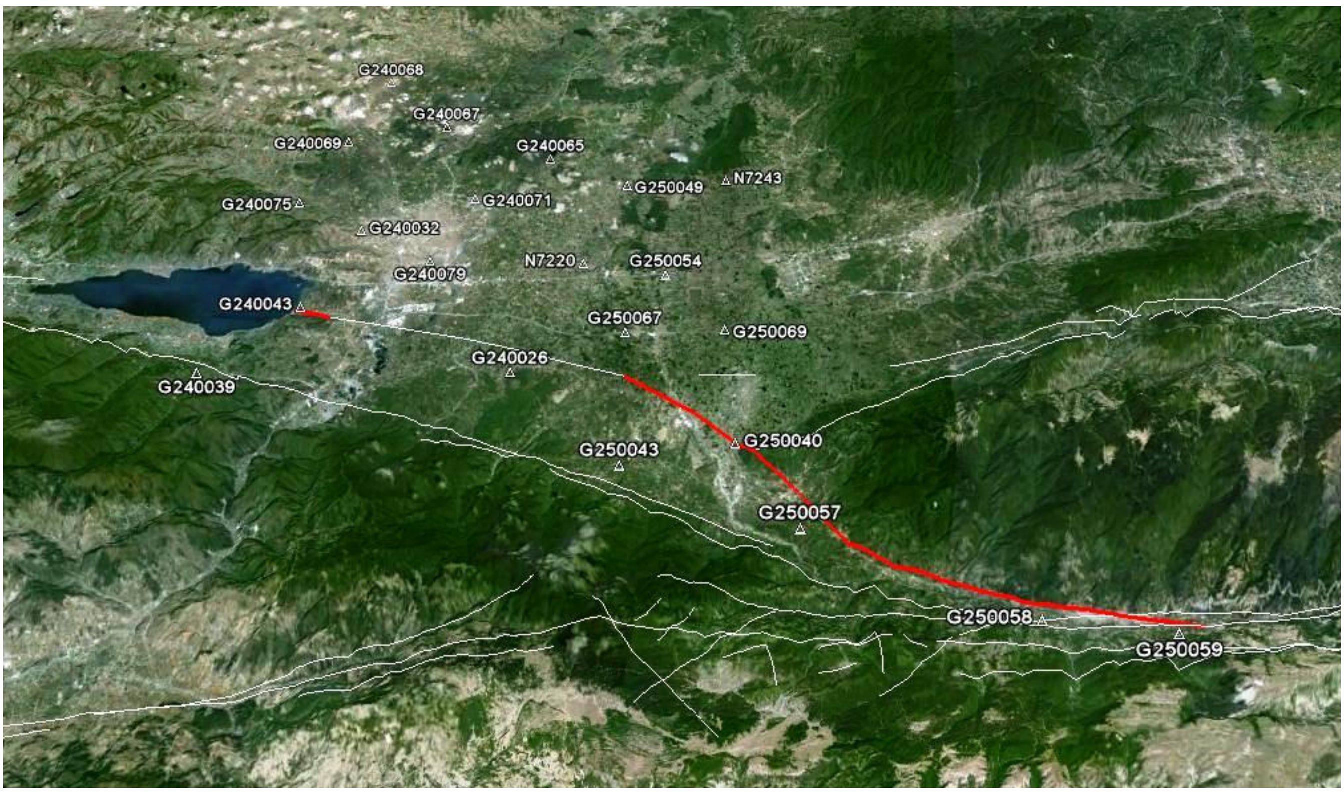

Fig. 7. Surface rupture in the Sakarya region. The red line shows the surface rupture defined by this study (satellite image from Google Earth).

30 km, see green rectangle on Fig. 2. Also, the post-seismic slip of the İzmit event between East Sapanca and Karadere was determined below the millimetre level by Ergintav et al. (2009). Thus, the displacement rates given above can be regarded as the co-seismic slip rates of the İzmit earthquake.

Last, the surface displacements obtained show that the surface rupture of the İzmit event runs to the main branch of the NAF displayed in Fig. 7. This result is contrary to the accepted belief; although the surface rupture in this region could not entirely be determined in the previous studies, the common view was that the rupture extended to the Karadere-Düzce segment.

4 Conclusions

The existence of the Sakarya GPS network has provided us with a valuable chance to obtain new results on the destruction caused by the earthquake sequence, eventhough it was not designed for monitoring tectonic activities in the region. As a first result, a comparison of between the 1998 and 2001 GPS observations yielded a maximum coseismic slip for the İzmit earthquake of between 2 m and 3 m in the south-eastern region of the geodetic network to the eastern shore of Sapanca Lake.

Secondly, the surface displacements obtained in this study shows that the Sapanca segment ruptured by the İzmit earthquake extends to the main branch of the NAF. This is also a new result since the former studies assumed that it was connected to the Karadere-Düzce segment.

Consequently, the results achieved in this study is completing an important gap ten years later related to the effects of the 1999 İzmit earthquake to the east of the Sapanca Lake.

Edited by: M. E. Contadakis
Reviewed by: P. H. Denys and another anonymous referee

References

Aliosmanoğlu, S.: Investigation of Geodetic Infrastructure Damages After Earthquake, Master thesis, Istanbul Technical University, Istanbul, Turkey, 2002 (in Turkish).

Barka, A.: The 17 August 1999 İzmit Earthquake, Science, 285, 1858–1859, 1999.

Cakir, Z., Barka, A., Chabalier, J. B., Armijo, R., and Meyer, B.: Kinematics of the November 12, 1999 (Mw=7.2) Düzce Earthquake Deduced from SAR Interferometry, Turk. J. Earth Sci., 12, 105–118, 2003a.

Cakir, Z., Chabalier, J. B., Armijo, R., Meyer, B., Barka, A., and Peltzer, G.: Coseismic and Early Postseismic Slip Associated with the 1999 İzmit earthquake (Turkey), from SAR Interferometry and Tectonic Field Observations, Geophys. J. Int., 155, 93–110, 2003b.

Çelik, R. N., Aliosmanoğlu, Ş., and Özlüdemir, M. T.: TUTGA, Depremler ve Büyük Ölçekli Çalimalar, TUJJB TUJK 2002 Bilimsel Toplantisi Tektonik ve Jeodezik Ağlar, İznik, 10-11-12 Ekim 2002.

Çelik, R. N., Aliosmanoğlu, Ş., and Özlüdemir, T.: Jeodezik Altyapidan Yararlanilarak Yer Kabuğu Yüzeyindeki Deprem Hasarlarinin Belirlenmesi, Deprem Sempozyumu, Kocaeli, 12–14 Mart 2003 (in Turkish).

Ergintav, S., McClusky, S., Hearn, E., Reilinger, R., Cakmak, R., Herring, T., Ozoner, H., Lenk, O., and Tari, E.: Seven years of postseismic deformation following the 1999, M=7.4 and M=7.2, Izmit-Düzce, Turkey earthquake sequence, J. Geophys. Res., 114, B07403, doi:10.1029/2008JB006021, 2009.

KOERI: Kandilli Observatory and Earthquake Research Institute, Turkey, available at: http://www.koeri.boun.edu.tr/depremmuh/eqspecials/duzce/duzceq.htm (last access: 2008), 2010.

Reilinger, R. E., Ergintav, S., Bürgmann, R., McClusky, S., Lenk, O., Barka, A., Gurkan, O., Hearn, L., Feigl, K. L., Cakmak, R., Aktug, B., Ozener, H., and Toksoz, M. N.: Coseismic and Postseismic Fault Slip for the 17 August 1999, M=7.5, İzmit, Turkey Earthquake, Science, 289, 1519–1523, 2000.

USGS: United States Geological Survey circular 1193, United State Government Printing Office, 2000.